ISSN: 2754-4966

Journal of Nanosciences Research & Reports

SCIENTIFIC Research and Community

Review Article

Open Access

Phase Composition and Structure of Ultrathin Nanocrystalline Cu-Ni Film Alloys

VB Loboda[1]*, SM Khursenko[1], VO Kravchenko[1], AV Chepizhnyi[1], VM Zubko[1] and AS Pastushenko[2]

[1]Faculty of Engineering and Technology, Sumy National Agrarian University, Sumy, Ukraine

[2]Berezhany Agrotechnical Institute, National University of Life and Environmental Sciences of Ukraine, Berezhany, Ukraine

ABSTRACT

The results of studying the morphology, crystal structure and phase composition of ultrathin Cu-Ni alloy films with thicknesses up to d = 10 nm and concentrations 0 < Cu < 100 at.% are presented.

Corresponding author

VB Loboda, Faculty of Engineering and Technology, Sumy National Agrarian University, Sumy, Ukraine.

Received: June 05, 2024; **Accepted:** June 24, 2024; **Published:** June 30, 2024

Keywords: Ultrathin Films, Island Films, Alloy Films, Phase Composition, Crystal Structure

Introduction

Much attention is paid to the study of physical phenomena occurring in thin films. This is due both to the wide practical use of films and to obtaining the information necessary to solve certain important problems in solid state physics and surface physics.

Along with studies of films made of pure metals (Cu, Ni), it is relevant and promising to study film alloys and film multilayer structures, which include Cu and Ni, and which differ from pure metal films in improved physicochemical, mechanical and operational characteristics [1-11]. Along with traditional film objects, in recent decades, a scientific direction has been formed related to the improvement of the service properties of massive metal samples by methods of creating layered structures in modified near-surface layers [12-14].

The properties of thin films, as a rule, differ significantly from the properties of bulk samples. Limiting the size of film objects in one of the directions leads to the appearance of so-called size effects, which are weakly expressed or not observed at all in the massive state. In the early stages of formation, thin films are not continuous. They are formed from small islands that may (or may not) be physically connected to each other depending on the thickness of the layer. The physical properties of island films differ significantly from the properties of both bulk metals and solid metal films.

This paper presents the results of a study of the morphology, crystal structure and phase composition of ultrathin Cu-Ni alloy films.

Experimental Details

Cu-Ni alloy films were obtained in a VUP-5M vacuum installation using a nitrogen oil vapor trap at a residual gas pressure of ~10-4 Pa and room temperature (300 K) the substrate temperature by the method of separate evaporation of components. The resistive heating method was used to evaporate copper, and the electron beam method was used to evaporate nickel. The films were condensed at a rate of $\omega \geq 1$ nm/s onto polished glass plates with preliminarily deposited copper contacts (to study electrical conductivity). For electron microscopic studies, NaCl cleavages with a thin layer of carbon were used (to eliminate the orienting effect of a single-crystal substrate).

To reduce the effect of the residual atmosphere on the purity of the film samples, the condensation of the films directly on the substrates was preceded by a long-term deposition of metals on the shutter screen. The purity of the starting metals was at least 99.98%.

The film thickness was measured by the microinterferometric method with an error of 5-10%. In the case of ultrathin (d < 10 nm) samples, as a rule, the film thickness is understood as the weight thickness determined from the deposition time and the known deposition rate ω. In this case, it is customary to speak of the effective film thickness.

The concentration of the film alloy components was determined by an X-ray microanalyzer using a REM-103-01 scanning electron microscope with an EDS attachment. Since the amount of substance in the studied film alloys is very small, the characteristic X-ray spectrum was excited by scanning a 300×300 μm section of the sample with an electron beam. This made it possible to obtain integrated data on the chemical composition of the film without overheating it with an electron beam (without introducing radiation damage).

The stabilization of the structural state of the alloy films and the study of the dependence of electrical resistance on temperature occurred during 3 "heating-cooling" cycles in the temperature

range 300-700 K. The temperature of the samples was controlled using a copper-constantan thermocouple with an error of ±10 K.

Electron microscopic and electron diffraction studies were carried out using a PEM-100-01 electron microscope.

Results and Discussion

Study of the Crystal Structure and Phase Composition of Films

As is known (see for example), the formation of the structure and properties of thin films obtained by vacuum evaporation is largely determined by the condensation conditions [15]. In this case, an important role is played by the material, purity, microrelief and temperature of the substrate, the degree of vacuum and the composition of the residual atmosphere, the rate of condensation of the substance, etc.

In an analysis was made of the influence of such parameters as the pressure and composition of the gases of the residual atmosphere (P), the condensation rate (ω), and the substrate temperature (Ts) on the phase composition and electrical properties of the films [16]. To describe the influence of the listed factors, the authors introduced the empirical parameter of condensation (α), which can be represented as:

$$\alpha = \frac{P}{\omega\sqrt{T_s}}.$$

Analyzing the data of a large number of works on the study of the phase composition of films obtained by vacuum condensation, we can conclude that purer samples (without impurity phases) can be obtained by increasing their condensation rate (at P = const) or by decreasing the pressure of the gases of the residual atmosphere (at ω = const). Thus, small values of α (low pressure or high rate of metal condensation) will correspond to better vacuum conditions. Then, the phase corresponding to bulk samples should form in the films with a higher probability. Conversely, at large values of α, the formation of impurity phases is possible.

At values of the condensation parameter $\alpha < 2.9\ 10^{-4}$ (Pa s) / (nm K½), nickel films have only the fcc phase with the lattice parameter a = 0.351 ± 0.001 nm, which is in good agreement with the value of the parameter a0 for massive samples [16]. For values of the condensation parameter $\alpha < 1.0\ 10^{-4}$ (Pa s)/(nm K½), copper films have only the fcc phase with the lattice parameter a = 0.361 ± 0.001 nm, which is also in good agreement with the value parameter a0 for massive samples [16]. Under our condensation conditions (P ~ 10^{-4} Pa, Ts = 300 K), the above criterion for the condensation parameter α was provided at a condensation rate of film alloys ω ≥ 1 nm/s.

Also, to reduce the effect of residual atmospheric gases on the physical properties of the samples under study, a well-known technique was used – preliminary spraying of metals on the damper and the inner surface of the working chamber (in this case, the composition of the residual atmosphere is significantly depleted in gases that actively interact with the condensate). The deposition time of the samples themselves was rather short (especially when obtaining island films).

In addition, copper-nickel film alloys, as noted in due to the presence of nickel, have increased resistance to corrosion even with prolonged exposure to atmospheric air [17].

The obtained films of copper-nickel alloys in the entire range of component concentrations have an fcc lattice with a parameter from a = 0.352 nm to a = 0.362 nm, depending on the concentration of the components. For bulk alloys 0.3524 < a0 < 0.3615 nm [18]. The formation of the fcc alloy occurs already at the stage of condensation, which is confirmed by electron diffraction (Figure 1).

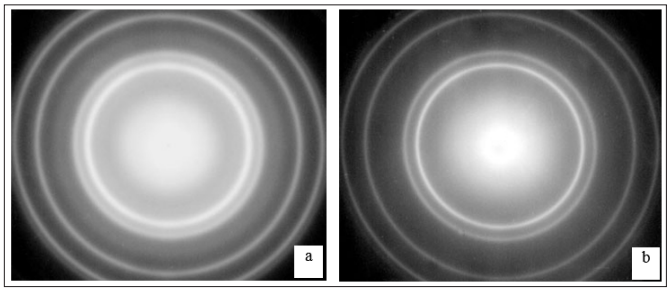

Figure 1: Electron Diffraction Images of Unannealed (a) and annealed to 700 K (b) Cu-Ni alloy films: d ≈ 1 nm, C_{Cu} = 50.3 at.%.

As can be seen from Figure 1, for unannealed films in the entire range of thicknesses and concentrations, the first line (111) is very wide. In this case, one gets the impression that it is double (this would take place in the case of the eutectic structure of the fcc Cu + fcc Ni alloy), but this is not so. The difference Δd111 = d111(Cu) – d111(Ni) = 0.009 nm is quite sufficient to observe the (111) Cu and (111) Ni lines separately by electron diffraction.

The results of studying the dependence of the lattice parameter of the Cu-Ni film alloy on the concentration of the components are shown in Figure 2. We note the fact that the lattice parameter in continuous alloy films is somewhat larger compared to bulk samples. This increase can be partly explained by the penetration of atoms from the residual atmosphere into the crystal lattice of the alloy, and partly by the fact that the atoms of one of the alloy components during condensation can occupy positions that do not correspond to an ordered alloy.

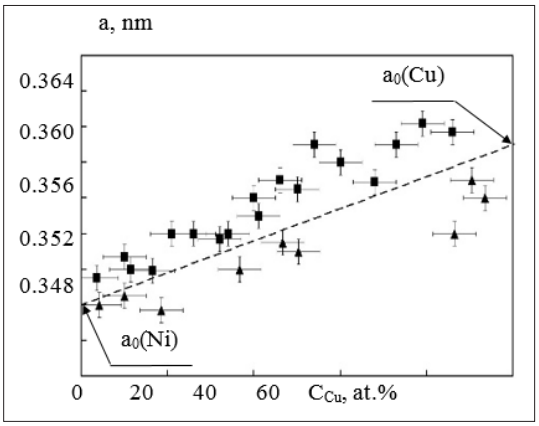

Figure 2: Concentration dependence of the fcc lattice parameter of Cu-Ni alloys (measurement temperature T = 300 K): ■ – continuous films; ▲ – island films; --- – Vegard's rule

As for bulk samples (dashed line in Figure 2), for Cu-Ni alloy films, an increase in the values of the lattice parameter from a = 0.353 nm to a = 0.362 nm is observed. For ultrathin Cu-Ni alloy samples with effective thicknesses d = 1-7 nm, the crystal lattice parameter is 0.002-0.003 nm less compared to bulk samples. There are a large number of experimental works in the literature (see, for example) in which it was shown that in island films of pure

fcc metals (including Ni and Cu, which make up the alloys under study), depending on the production conditions, the parameter lattice parameter can be either smaller or larger than the bulk metal lattice parameter, increasing or decreasing with increasing island size [15, 16, 19, 20]. However, under conditions where the influence of gas impurities is minimized, the lattice parameter always decreases with decreasing particle size.

When explaining the reasons for this phenomenon, one proceeds either from the presence of an additional (Laplace) pressure arising due to the small radius of curvature of a nanoparticle or from an increased (compared to a macroscopic sample) concentration of surface and near-surface vacancies in nanoparticles [16, 19].

Investigation of the Microstructure of Ultrathin Films

Condensation of ultrathin film samples of Cu-Ni alloys was carried out at room temperature of the substrate. It is known that condensation of a molecular beam on neutral substrates occurs only under the condition that the substrate temperature Ts is less than a certain value Tc (critical condensation temperature). In this case, depending on the rate of condensation ω, the temperature Tc can be either lower than the melting temperature of bulk samples Tm or higher than this temperature [15]. In accordance with the concepts of the mechanism of formation of thin films that have developed on the basis of theoretical and experimental studies in the literature it is customary to distinguish the following regimes of condensate growth:

Layer-by-Layer (Frank-van der Merwe mode)

Is realized if the atoms of the deposited substance bind to the atoms of the substrate (as a rule, single-crystal, with a close lattice parameter) more strongly than to each other; in this case, on the substrate, the construction of a monolayer of a substance is first completely completed, on which a second monolayer, a third, etc. are formed.

Island (Volmer-Weber Mechanism)

Is realized in the case when the atoms of the deposited substance are bound to each other more strongly than with the atoms of the substrate (usually neutral). In this case, small nuclei formed on the surface of the substrate grow, turning into large islands of the condensed phase. Upon reaching a certain average thickness (critical thickness), which depends on the kinetics of the condensation process, contacts appear between individual islands and a characteristic labyrinth structure with channels appears. After the channels are filled, a continuous film is formed.

Intermediate (The Stranski-Krastanov Mode)

In which layer-by-layer growth occurs first, then, after one or two layers are filled, the island growth regime begins. The main reason for the change in growth mechanisms is the change in the lattice parameter when the next layer is filled, which leads to a violation of the conditions for implementing the mechanism of layer-by-layer growth and ensures the fulfillment of the island growth criterion.

The process of formation of Cu-Ni film alloys at the initial stages of growth can be traced in Figure 3, which shows micrographs of samples of different thicknesses.

An analysis of these micrographs for ultrathin Cu-Ni alloys suggests that in this case an island growth regime is realized. At the same time, in freshly condensed ultrathin Cu-Ni films with an effective thickness d ≈ 1-2 nm, regardless of composition, almost the same structure was observed with an average size of individual islands 1.5-2 nm. Upon reaching the effective thickness d ≈ 3 nm, which is most likely critical (percolation threshold) for Cu-Ni film alloys, the so-called classical labyrinth structure with irregularly shaped islands connected to each other and channels between the islands was observed on electron microscopic images. about the same width. A further increase in the effective thickness of the films to d ≈ 10 nm structurally manifested itself only in an increase in the density of islands and a decrease in the number of channels due to their gradual filling.

Experimental studies (see, for example, and the literature cited therein) show that, in the case of an island growth mechanism, isolated islands can be either individual microcrystals or liquid drops that have already crystallized [16]. Thus, during island growth, two condensation mechanisms are possible:

- The formation of islands of the crystalline phase directly from the vapor of the condensed substance (the "vapor → crystal" mechanism).
- The formation of islands of the liquid phase, which can later crystallize (the "vapor → liquid" mechanism).

As can be seen, all the obtained films at thicknesses up to 10 nm are island, with the size of individual islands from 0.5-2 nm in unannealed (Figure 3a) to 20 nm in annealed (Figure 3b-f) films, depending on the thickness of the sample. It should be noted that only in the thinnest samples (d ≈ 1 nm, Figure 3b), as a result of annealing to 700 K, an insignificant amount of Cu2O oxides appears, which are fixed electron diffraction in the form of weak additional lines (110, 111, and 220).

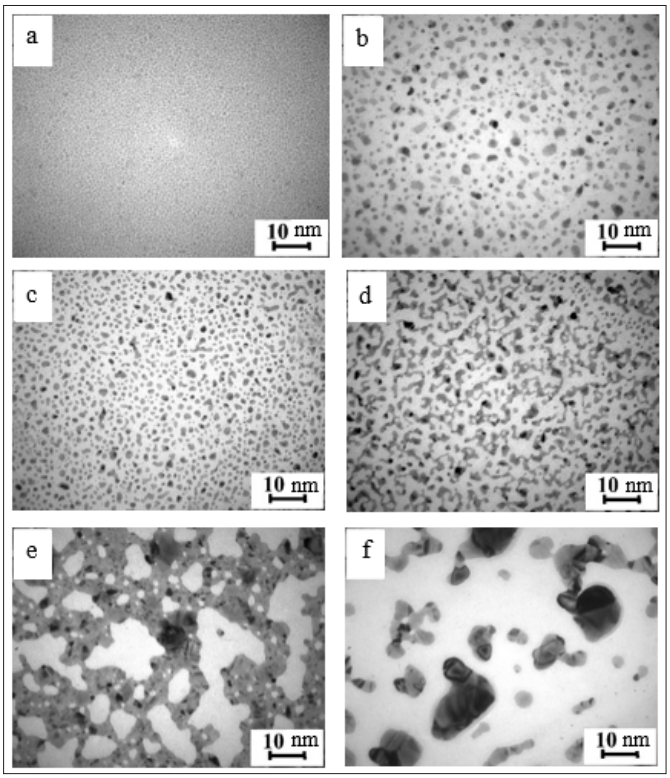

Figure 3: Microstructure of unannealed (a) and annealed up to 700 K (b-f) ultrathin Cu-Ni alloy films of different thicknesses: d = 1 nm, C_{Cu} = 50.3 at.% (a, b); d = 2.5 nm, C_{Cu} = 36.7 at.% (c); d = 3.5 nm, C_{Cu} = 86.5 at.% (d); d = 6 nm, C_{Cu} = 90.5 at.% (e); d = 6.5 nm, C_{Cu} = 9.8 at.% (f).

Since the condensation was carried out on a neutral nonorienting substrate (carbon film) at Ts ≈ 300 K < ⅓Tm (Ts is the substrate temperature, Tm is the melting temperature of the alloy of a

given concentration (1400 K < Tm < 1700 K)) and the diffusion mobility of atoms in the islands was difficult, then in unannealed films, regardless of the thickness and composition, almost the same structure was observed (Figure 3a). In this case, the smallest islands have an irregular shape, and the gaps between them acquire the characteristic shape of channels with approximately the same width (classical "labyrinth" structure). An increase in the film thickness is structurally manifested only in an increase in the density of islands. On the other hand, subsequent annealing to T = 700 K leads to a significantly different morphological state of the film, depending on its thickness. At thicknesses d ≈ 1-3 nm (Figure 3b, c), the islands are simply enlarged (migratory coalescence) and the total number of islands decreases significantly. At d ≈ 3-4 nm (Figure 3d), a characteristic "bridge" structure is formed.

The most significant transformations upon annealing are experienced by films of approximately the same thickness, d ≈ 6 nm, but with different component concentrations (Figure 3e,f). At CCu = 90.5 at.%, the film becomes electrically continuous (Figure 3f), while at CCu = 9.8 at.% it remains island-like (Figure 3f). Separate islands of complex shape with a clear facet have dimensions of more than 10-15 nm. At the same time, crystals are visible inside the particles (even rather small ones), the shape, size and number of which are not constant. Their appearance can be associated with the onset of recrystallization processes. The unification of the islands themselves into larger ones (Figure 3f) obviously occurs according to the mechanism of "liquid-like" coalescence. The appearance of the "flattened" structure shown in Figure 3f can be explained by the manifestation of the autocoalescence effect.

Conclusion

The study of the phase and elemental composition of film alloys made it possible to establish the following patterns:

- All studied ultrathin Cu-Ni alloy films have an fcc alloy lattice with a parameter from 0.352 nm to 0.362 nm, depending on the content of the components.
- The investigated films are structurally discontinuous, have an island structure (for unannealed samples, the sizes of individual islands are 0.5-2 nm; for samples annealed to 700 K, up to 20 nm, depending on the film thickness).
- The percolation threshold of the labyrinth structure (the minimum film thickness above which the labyrinth structure appears) is approximately 3 nm.

References

1. VK Soni, S Sanyal, SK Sinha (2020) Phase evolution and mechanical properties of novel FeCoNiCuMox high entropy alloys. Vacuum 174: 109173.
2. X Hua, J Li, H Liu, Z Yang, SF Liu (2021) Preparation of Cu2Se thin films by vacuum evaporation and hot-pressing. Vacuum 185: 109947.
3. G Li, G Song, N Wang (2022) Influence of Cu content on the phase composition and thermoelectric properties of deposited Cu-Se films. Surfaces and Interfaces: 101651.
4. OV Pylypenko, IM Pazukha, AS Ovrutskyi, LV Odnodvorets (2016) Electrophysical and magnetoresistive properties of thin film alloy Ni80Fe20. Journal of Nano- and Electronic Physics 8: 03022.
5. Y Bereznyak, L Odnodvorets, D Poduremne, I Protsenko, Y Shabelnyk (2018) High-entropy film alloys: Electrophysical and magnetoresistive properties. Springer Proceedings in Physics 210: 17-24.
6. YO Shkurdoda, AM Chomous, YM Shabelnyk, VB Loboda, SM Khursenko (2020) Method of Production and Structural-phase State of Medium-entropy Equiatomic FeNiCoCu Film Alloy. Proceedings of the IEEE 10th International Conference on "Nanomaterials: Applications and Properties: 9309616.
7. DI Saltykov, SI Protsenko, IM Pazukha, YO Shkurdoda (2020) Concentration and heat treatment effects on magnetoresistive properties of three-layer film systems based on FexCo100-x and Cu. Thin Solid Films 716: 138422.
8. OV Bezdidko, SA Nepijko, YO Shkurdoda, YM Shabelnyk (2021) Structure and Magnetoresistive Properties of Three-layer Films Co(1–x)Crx/Cu/Co. Journal of Nano- and Electronic Physics 13: 1-4.
9. VB Loboda, VM Kolomiets, SM Khursenko, YO Shkurdoda (2014) The electrical conductivity of the three-layer polycrystalline films Co/Ag(Cu)/Fe in the conditions of atoms interdiffusion. Journal of Nano- and Electronic Physics 6: 04032.
10. VB. Loboda, YuO Shkurdoda, VO Kravchenko, SM Khursenko, VM Kolomiets (2011) Structure and magnetoresistive properties of polycrystalline Co/Cu/Co films. Metallofizika i Noveishie Tekhnologii 33: 161-169.
11. VB Loboda, VM Kolomiets, YuO Shkurdoda, VO Kravchenko, LV Dekhtyaruk (2012) Structure and magnetoresistive properties of nanocrystalline film systems based on Co, Fe, Ag, and Cu. Metallofizika i Noveishie Tekhnologi 34: 1043-1055.
12. AD Pogrebnjak, AG Lebed, Yu F Ivanov (2001) Modification of single crystal stainless steel structure (Fe-Cr-Ni-Mn) by high-power ion beam. Vacuum 63: 483-486.
13. AD Pogrebnjak, VT Shablya, NV Sviridenko, SV Plotnikov, MK Kylyshkanov (1999) Study of deformation states in metals exposed to intense-pulsed-ion beams (IPIB). Surface and Coatings Technology 111: 46-50.
14. VI Lavrentiev, AD Pogrebnjak (1998) High-dose ion implantation into metals. Surface and Coatings Technology 99: 24-32.
15. Yu F Komnik (1979) Physics of Metal Films. Dimensional and Structural Effects. Moscow: Atomizdat (in Russian).
16. https://ui.adsabs.harvard.edu/abs/1979MAtom....R....K/abstract.
17. NT Gladkikh (2004) Surface phenomena and phase transformations in condensed films. Khar'kov: KHNU im. VN Karazina (in Russian).
18. AI Kostrzhitsky, OV Lebedinsky (1987) Multicomponent vacuum coatings. Moscow: Mashinostroenie (in Russian).
19. V G Bar'yakhtar (1996) Solid State Physics: Encyclopedic Dictionary. Kyiv: Naukova dumka 1: 531. (in Russian).
20. SA Nepiyko (1985) Physical properties of small metal particles. Kyiv: Naukova dumka (in Russian).
21. ID Morokhov, LI Trusov, SP Chizhik (1977) Ultrafine metallic medium. Moscow: Atomizdat (in Russian).